Supporting Information

Antibacterial and Immunomodulatory Activities of Physiologically Stable, Self-Assembled Peptide Nanoparticles

Nauman Nazeer[1], Jeffrey R. Simmons[2], Jan K. Rainey[2-4] Juan Carlos Rodriguez- Lecompte[5], Marya Ahmed[1,6]

Department of Chemistry University of Prince Edward Island, Charlottetown, Prince Edward Island, Canada, C1A 4P3[1], Department of Biochemistry & Molecular Biology[2], Department of Chemistry[3], School of Biomedical Engineering, Dalhousie University, Halifax, Nova Scotia B3H 4R2, Canada[4]; Department of Pathology and Microbiology, Atlantic Veterinary College[5], Faculty of Sustainable Design Engineering[6]; University of Prince Edward Island, Charlottetown, Prince Edward Island, Canada, C1A 4P3

Corresponding email address: marahmed@upei.ca

Table S1. Particle size and zeta potential of FC-DSNs at different FC:peptide weight ratios.

Sample	Particle size (nm)	Zeta Potential (mV)
DSN aggregates	282.03 ± 100.41	14.14 ± 1.08
FC-DSNs (1:4)	130.96 ± 1.58	8.45 ± 1.23
FC-DSNs (1:2)	113.74 ± 20.32	-0.60 ± 0.04
FC-DSNs (1:1)	159.99 ± 11.86	-15.98 ± 2.88

Table S2. Determination of Cα and Hα amino acid secondary structure through comparison of chemical shifts relative to random coil shifts for amino acids in 100% DMSO.

#	Residue	$\Delta\delta$Cα	Threshold Helix	Threshold Sheet	Structure	$\Delta\delta$Hα	Threshold Helix	Threshold Sheet	Structure
*	Cys	-1.355	>1.3	<-0.1	Sheet	-0.117	<-0.16	>0.22	Helix
*	Arg	-0.536	>1.3	<-0.1	Coil	-0.079	<-0.16	>0.22	Coil
*	Phe	-1.375	>1.3	<-0.1	Sheet	0.051	<-0.16	>0.22	Coil
*	Lys	-0.701	>1.3	<-0.1	Sheet	-0.12	<-0.16	>0.22	Helix
*	Phe	-1.607	>1.3	<-0.1	Sheet	-0.002	<-0.16	>0.22	Coil
*	Arg	-0.713	>1.3	<-0.1	Sheet	-0.11	<-0.16	>0.22	Helix
*	Ile	-0.931	>1.3	<-0.1	Sheet	-0.085	<-0.16	>0.22	Coil
8	Val	-0.565	>1.3	<-0.1	Coil	-0.062	<-0.16	>0.22	Coil
*	Ile		>1.3	<-0.1			<-0.16	>0.22	
*	Cys			<-0.1			<-0.16	>0.22	

* indicates ambiguous assignments

Table S3. Determination of Cβ amino acid secondary structure through comparison of chemical shifts relative to random coil shifts for amino acids in 100% DMSO.

#	Residue	ΔδCβ	Threshold Helix	Threshold Sheet	Structure
*	Cys		<-0.3	>0.2	
*	Arg	-0.694	<-0.3	>0.2	Coil
*	Phe	1.761	<-0.3	>0.2	Sheet
4	Lys	-0.38	<-0.3	>0.2	Coil
*	Phe	2.042	<-0.3	>0.2	Sheet
*	Arg	-0.676	<-0.3	>0.2	Coil
*	Ile	-1.112	<-0.3	>0.2	Helix
8	Val	-0.552	<-0.3	>0.2	Coil
*	Ile	-0.705	<-0.3	>0.2	Helix
*	Cys		<-0.3	>0.2	

* indicates ambiguous assignments

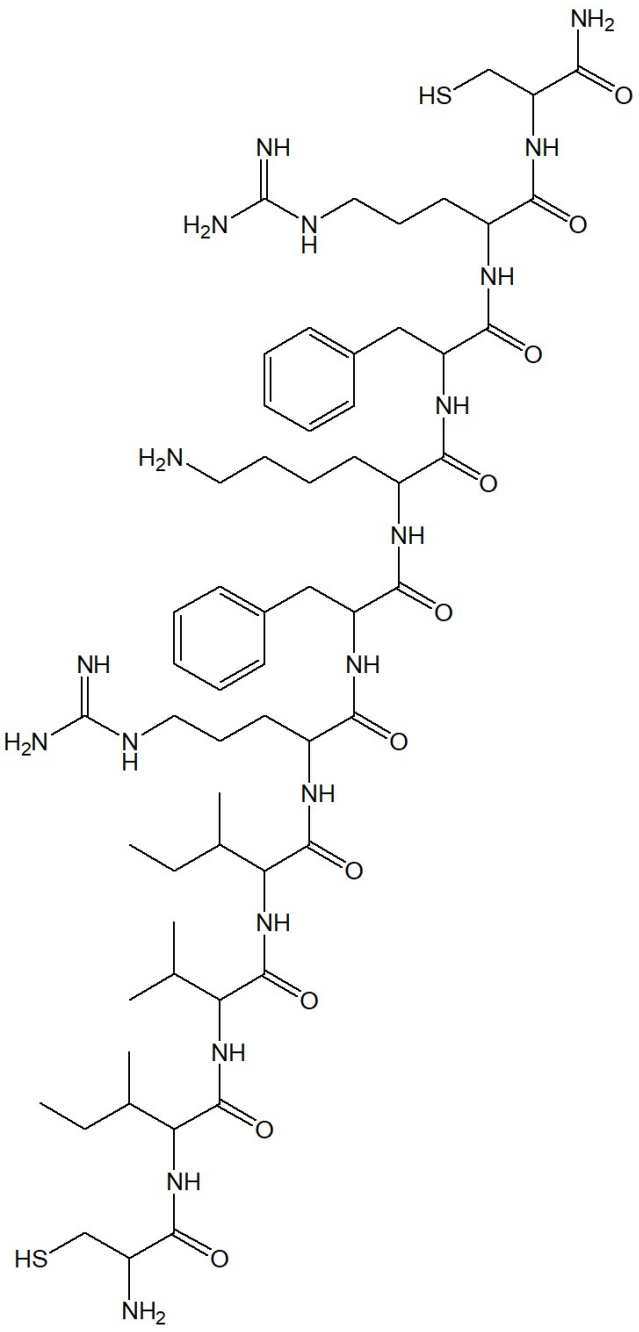

Figure S1. Chemical structure of CRFKFRIVIC peptide.

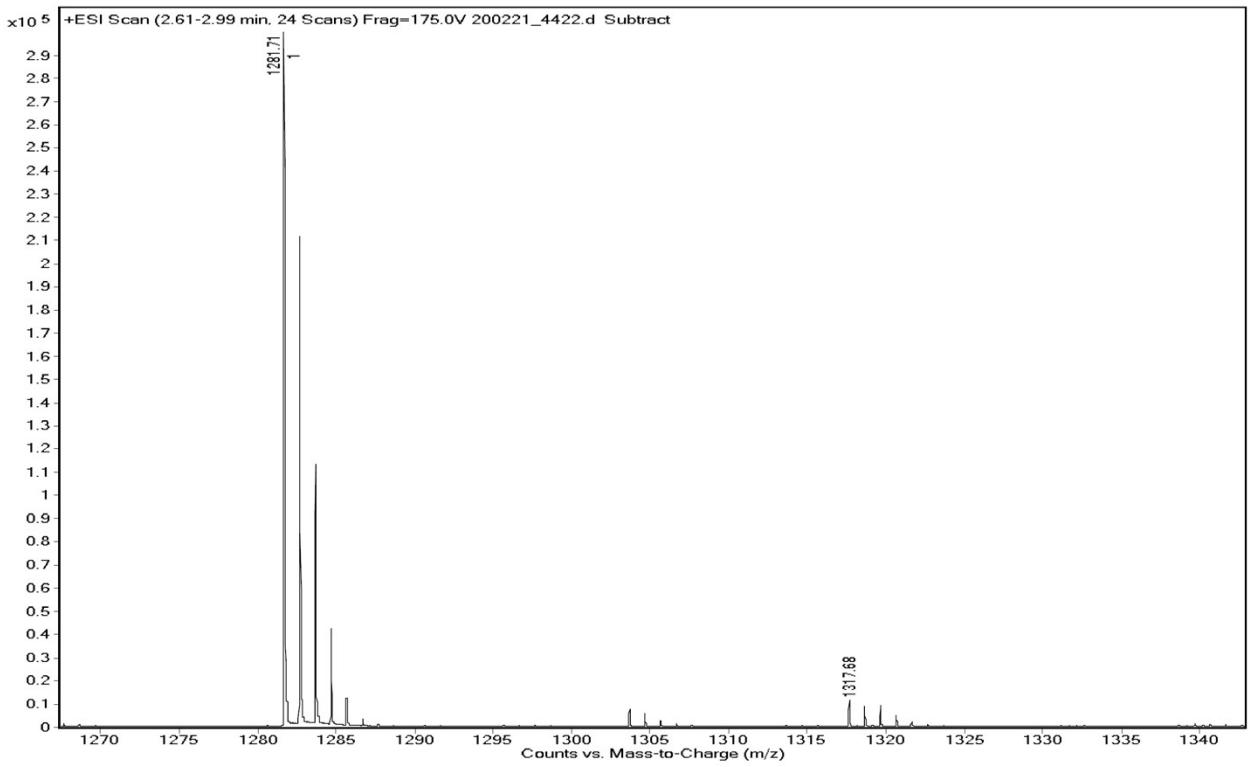

Figure S2. Mass spectrometry data for CRFKFRIVIC peptide.

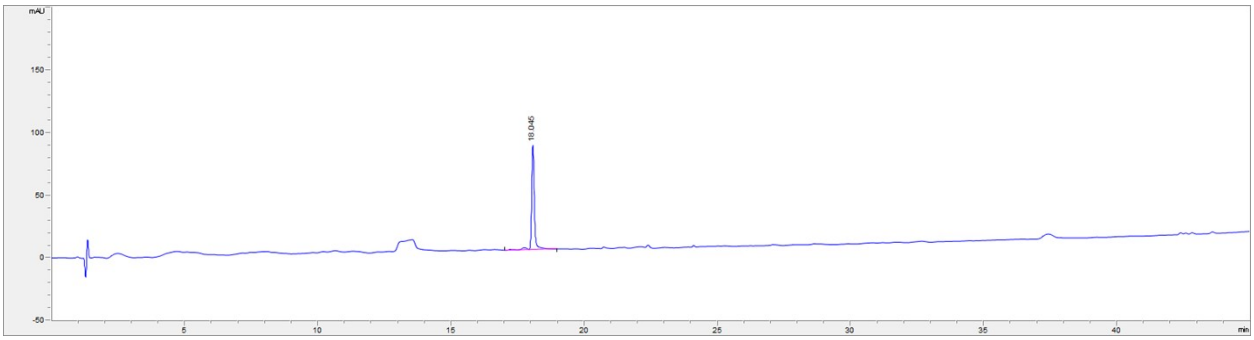

Figure S3. RP-HPLC chromatogram of CRFKFRIVIC peptide.

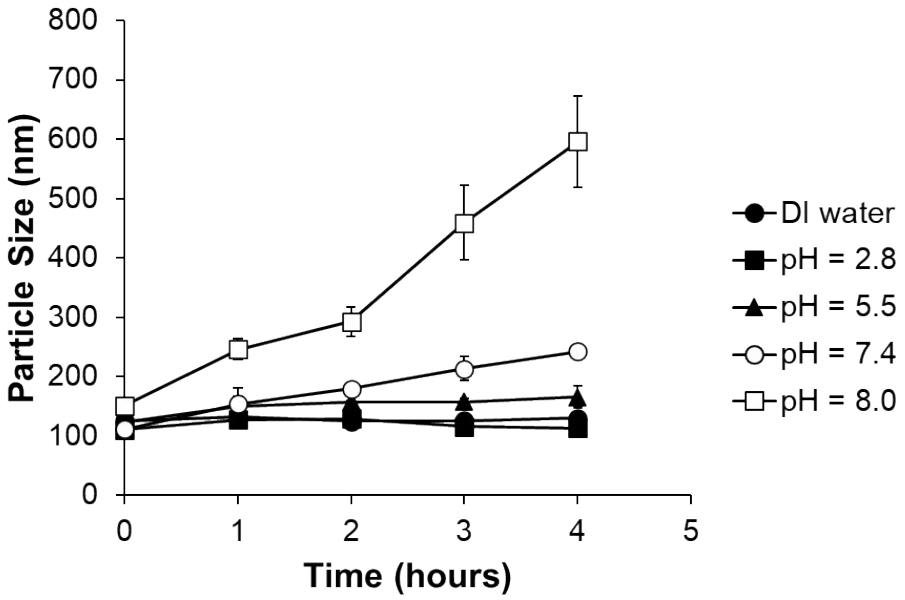

Figure S4. Effect of pH on particle size of FC-DSNs.

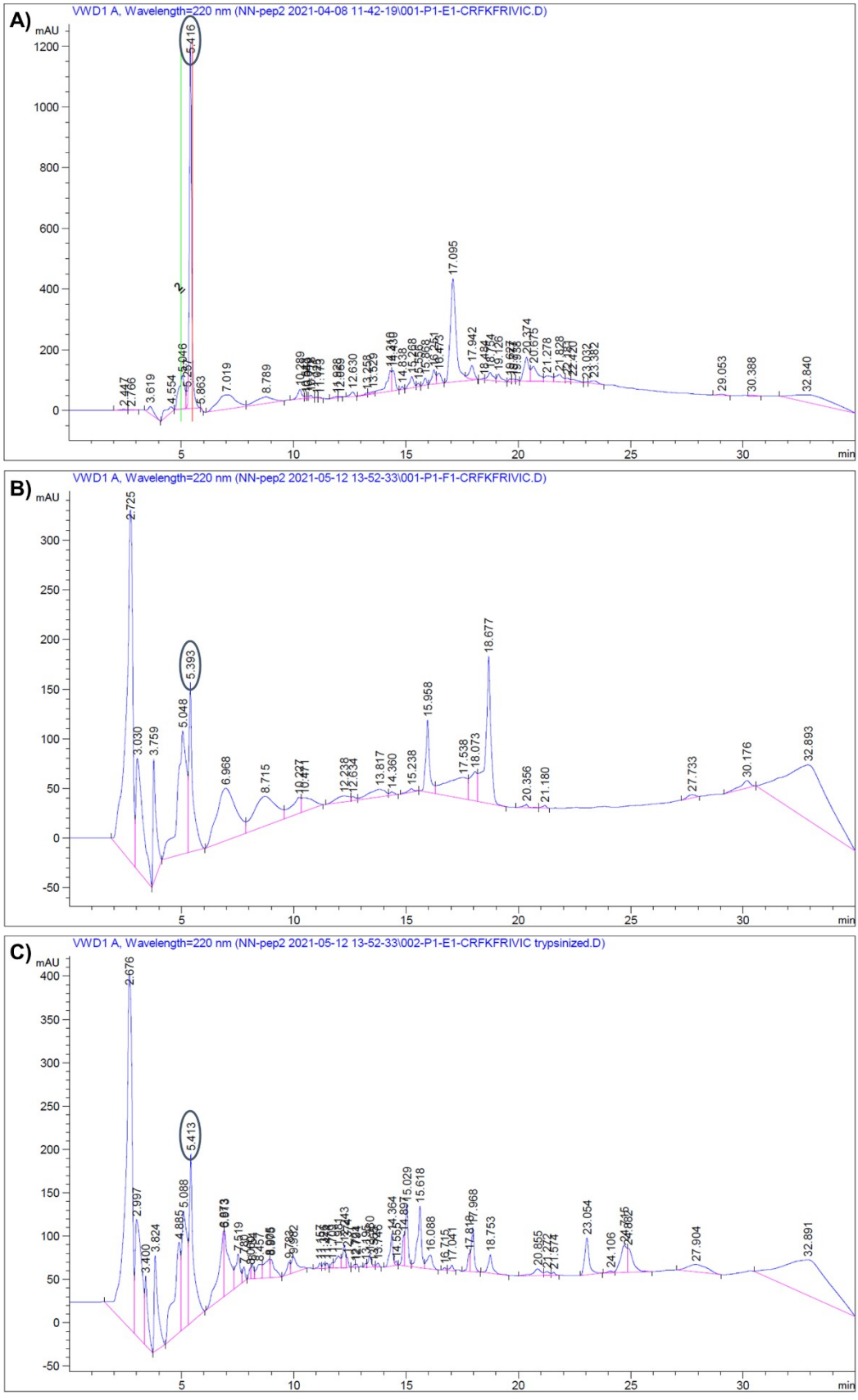
A)
VWD1 A, Wavelength=220 nm (NN-pep2 2021-04-08 11-42-19\001-P1-E1-CRFKFRIVIC.D)
mAU
5.416
17.095
B)
VWD1 A, Wavelength=220 nm (NN-pep2 2021-05-12 13-52-33\001-P1-F1-CRFKFRIVIC.D)
mAU
2.725
5.393
18.677
C)
VWD1 A, Wavelength=220 nm (NN-pep2 2021-05-12 13-52-33\002-P1-E1-CRFKFRIVIC trypsinized.D)
mAU
2.676
5.413
min

Figure S5. RP-HPLC chromatograms of **A)** DSNs in water:acetonitrile solution with 0.1% TFA, **B**) DSNs in Tris-buffer **C)** DSNs in Tris-buffer in the presence of trypsin-EDTA.

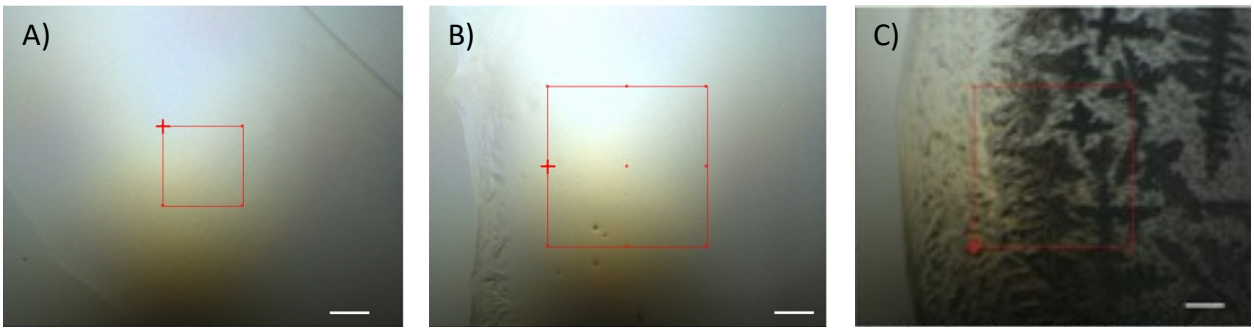

Figure S6. Optical microscopy images of thin films cast from **(A)** CRFKFRIVIC peptide in DMSO; **(B)** β-CD-DSNs; and **(C)** FC-DSNs. Red boxes and points are illustrative of sampling positions at which FTIR spectra were acquired for a given sample; scale bars are 50 μm.

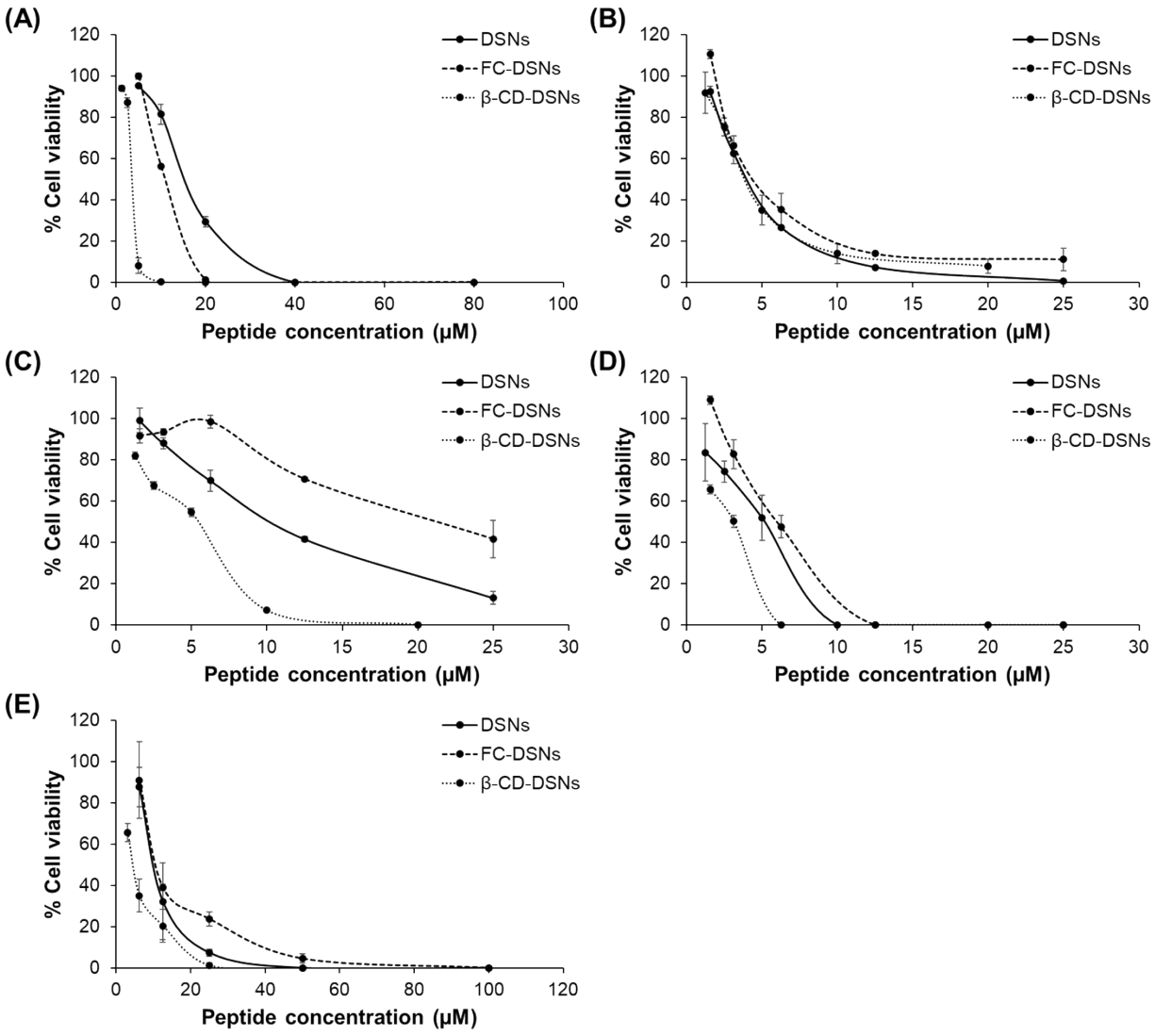

Figure S7. Concentration-dependent antibacterial activity of DSNs, FC-DSNs, and β-CD-DSNs after 4-hour treatment against **(A)** *E. coli* (ATCC 25922); **(B)** *S. aureus* (ATCC 25923); **(C)** *S. enterica* (ATCC 13076); **(D)** *L. monocytogenes* (ATCC 19115); and **(E)** *B. subtilis* (ATCC 6051).

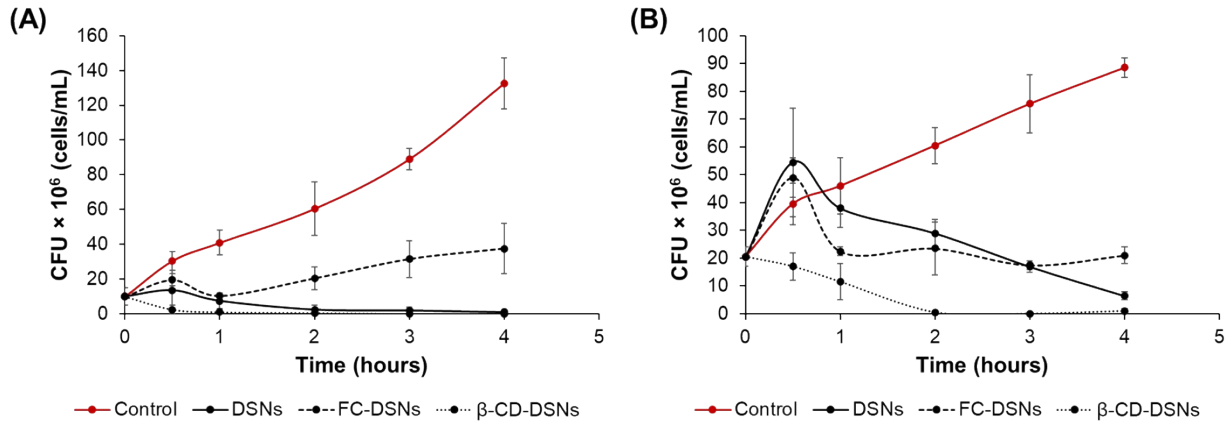

Figure S8. Time-dependent antibacterial activity of DSNs, FC-DSNs, and β-CD-DSNs at a peptide concentration of 25 μM against **(A)** *E. coli* (NEB 5α) and **(B)** *B. subtilis* (ATCC 6051).

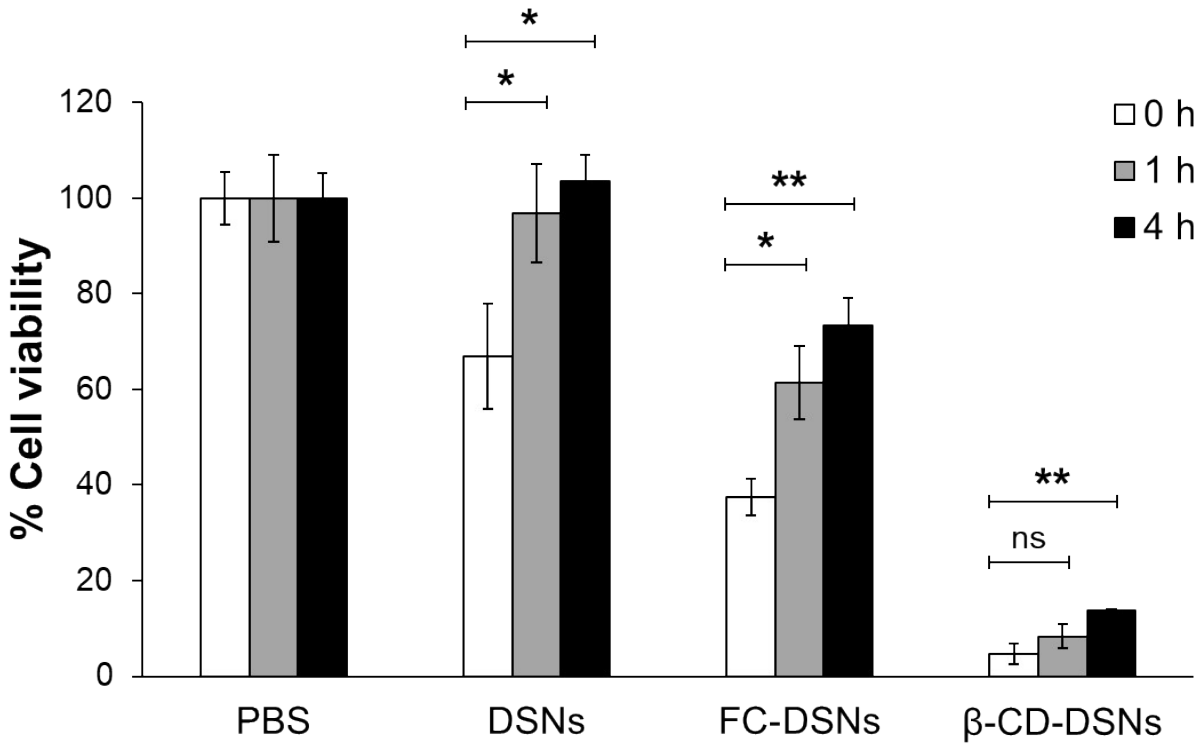

Figure S9. Antibacterial activity of DSNs and its macromolecular analogues in the presence of serum proteins. * indicates p-value < 0.05, ** indicates p-value < 0.01, and ns indicates no statistically significant difference.

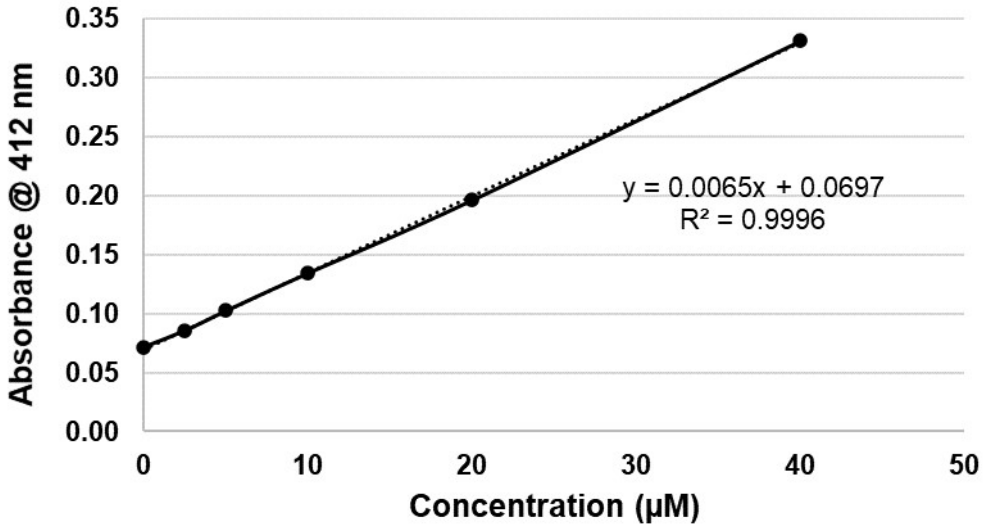

Sample	Mean Absorbance @ 420 nm
Blank	0.0718 ± 0.0004
DSNs (40 µM)	0.087 ± 0.0002

Figure S10. Calibration of L-cysteine hydrochloride monohydrate by Elman's assay.

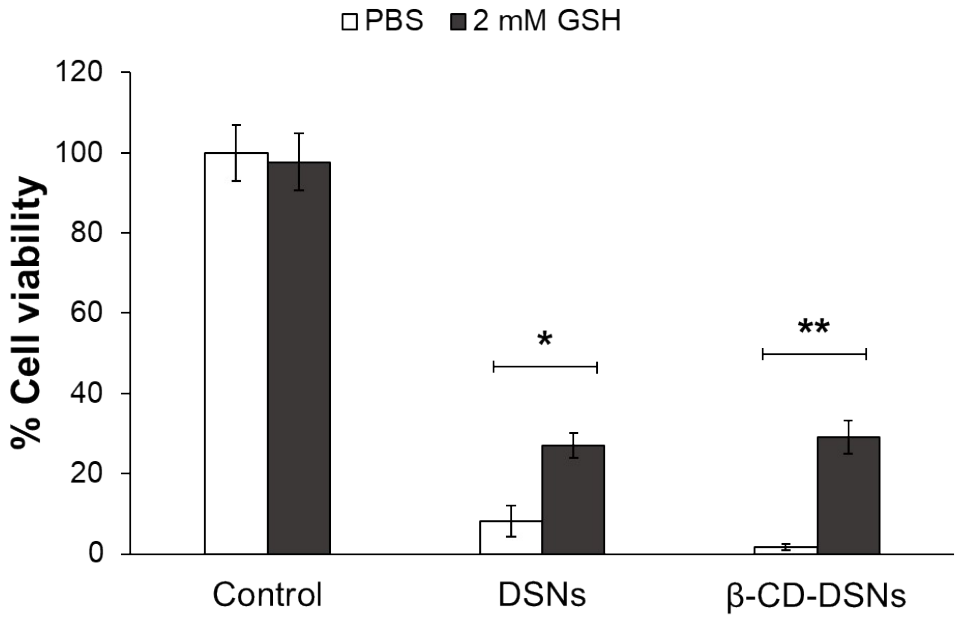

Figure S11. Antibacterial activity of DSNs and β-CD-DSNs in the presence of 2mM GSH. * indicates p-value < 0.05 and ** indicates p-value < 0.01.

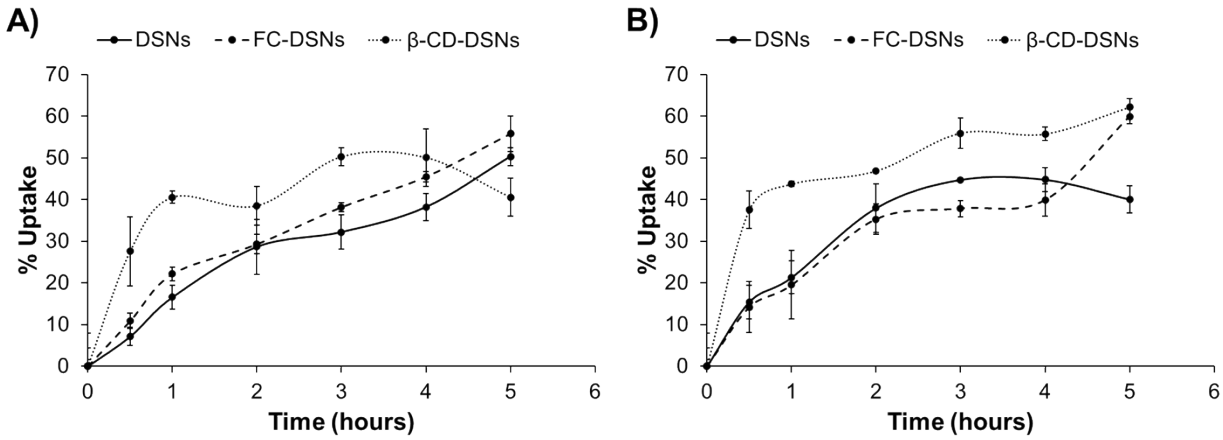

Figure S12. Uptake of TAMRA-labelled peptide nanoparticles in **(A)** *E. coli* and **(B)** *B. subtilis*.

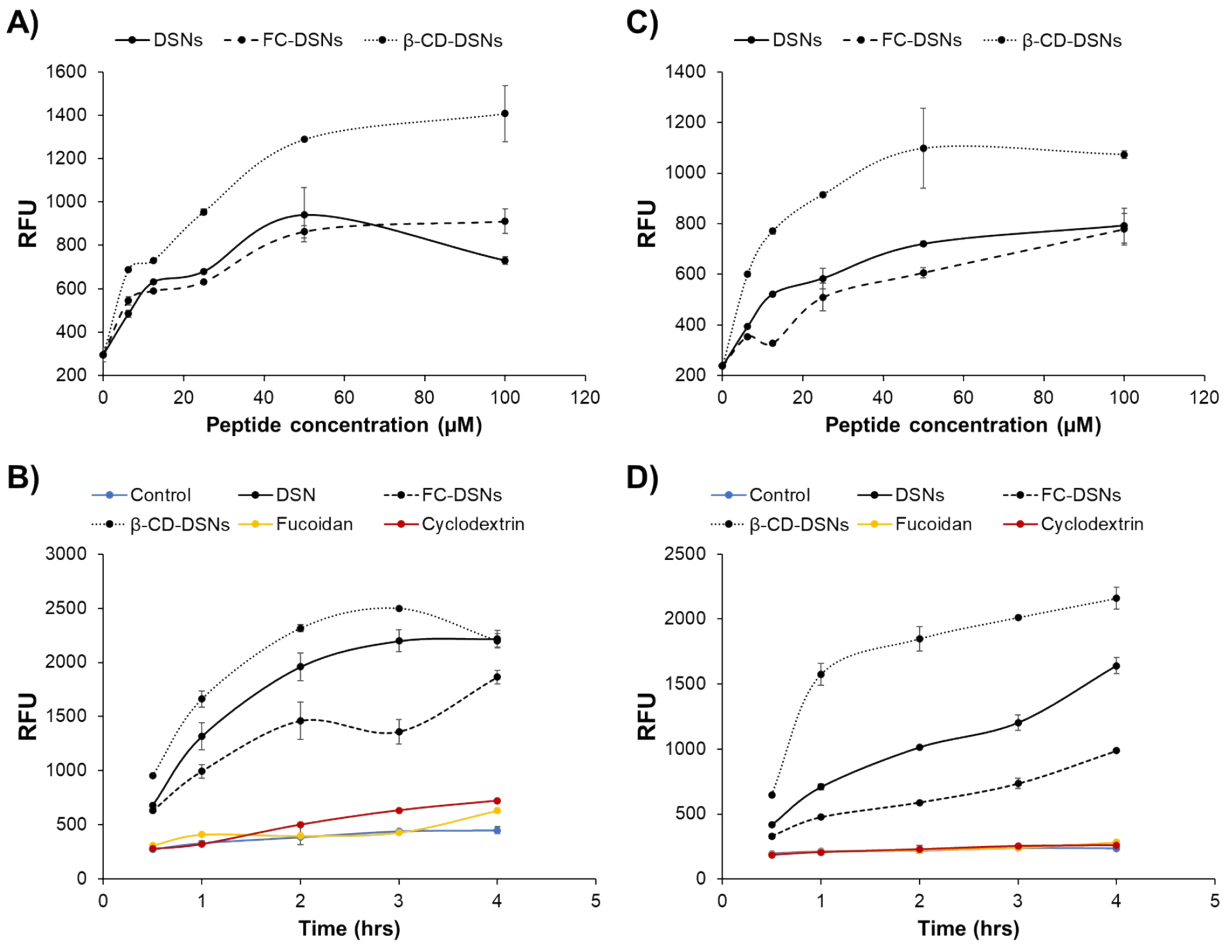

Figure S13. Uptake of CF in **(A-B)** *E. coli* and **(C-D)** *B. subtilis*. A and C shows concentration-dependent change in membrane permeability after 30 minutes of incubation with samples. B and D shows time-dependent change in membrane permeability after treatment with 25 μM of DSNs and equimolar concentrations of FC-DSN and β-CD-DSN.

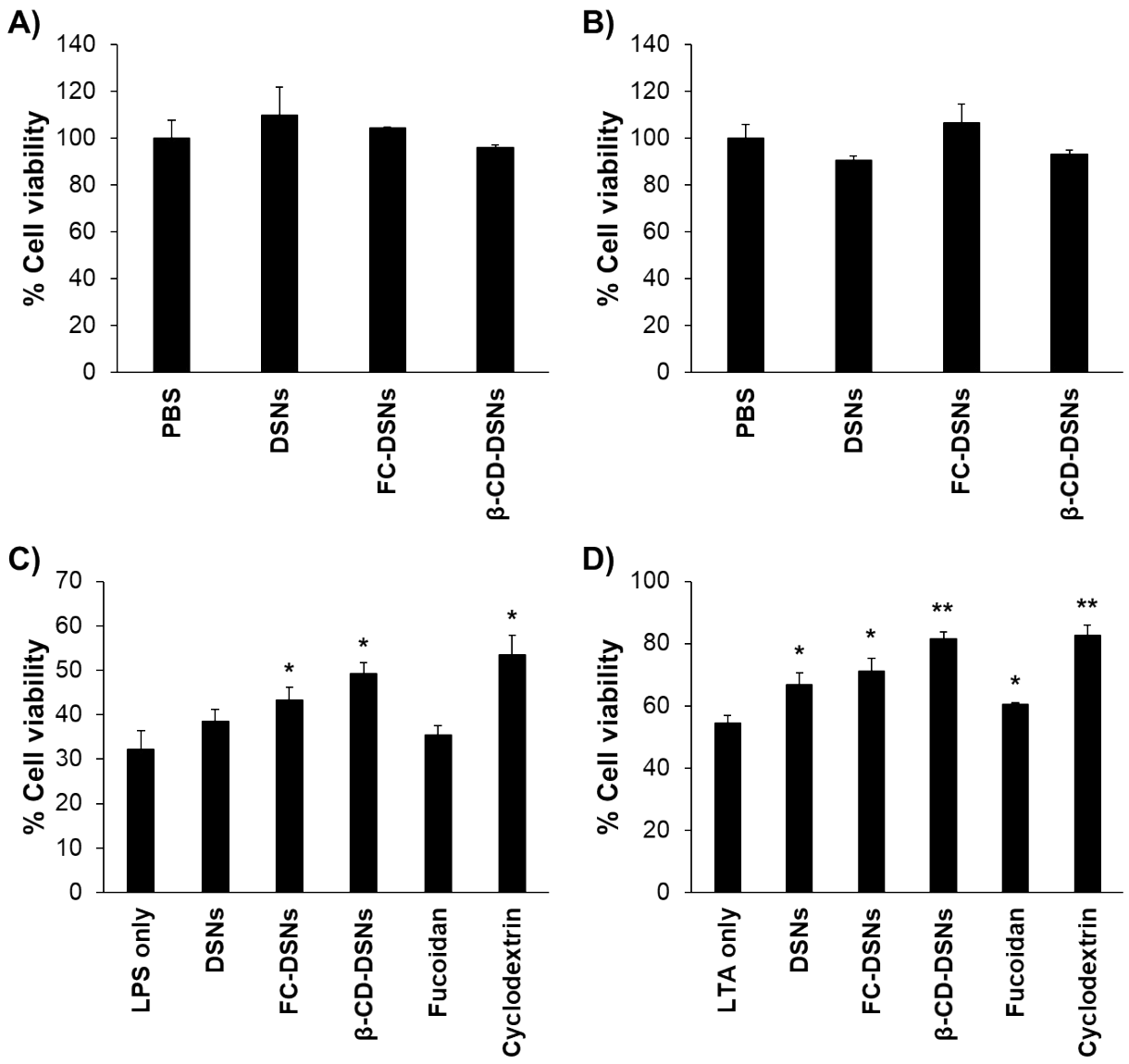

Figure S14. Cell viability of **(A)** DF-1 chicken fibroblasts; **(B)** Caco-2 cells; **(C)** Caco-2 cells treated with 100 µg/mL LPS; and **(D)** Caco-2 cells treated with 100 µg/mL LTA. * indicates p-value < 0.05 compared to control treatment and ** indicates p-value < 0.01 compared to control treatment.

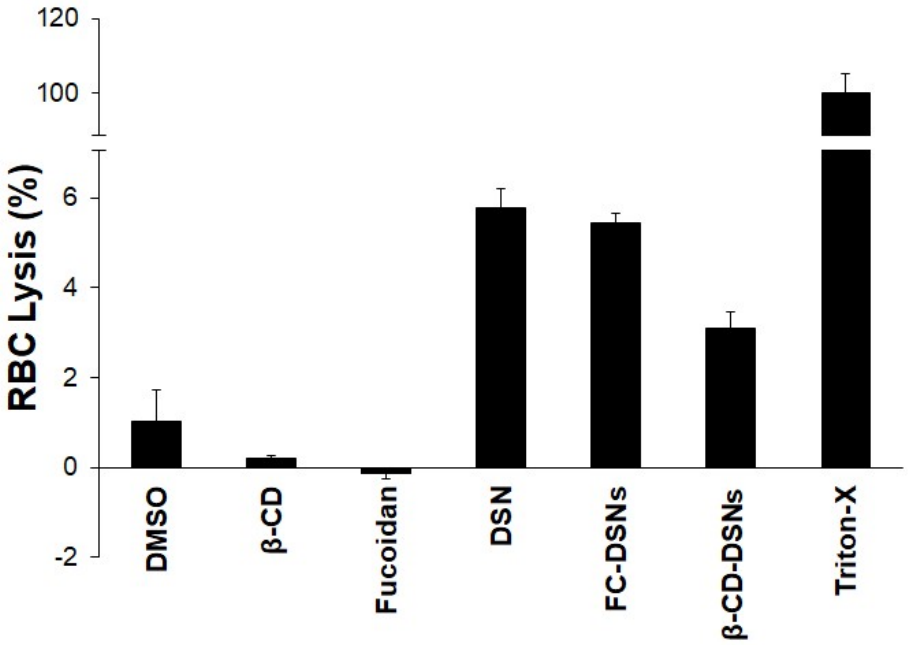

Figure S15. Hemolytic activity of peptide-based nanoparticles.